Efficient Plasma Source Providing Pronounced Density Peaks in the Range of Very Low Magnetic Fields

doi: 10.1063/1.1815071

Efficient plasma source providing pronounced density peaks in the range of very low magnetic fields

G. Sato,[a] W. Oohara, and R. Hatakeyama
Department of Electronic Engineering, Tohoku University, Sendai 980-8579, Japan

(Received 2 June 2004; accepted 8 September 2004)

Radio-frequency discharges are performed in low magnetic fields (0–10 mT) using three types of helicon-wave exciting antennas with the azimuthal mode number of $|m|=1$. The most pronounced peak of plasma density is generated in the case of a phased helical antenna at only a few mT, where the helicon wave with $m=+1$ is purely excited and propagates. An analysis based on the dispersion relation well explains the density-peak phenomenon in terms of the correspondence between the antenna one-wavelength and the helicon wavelength, bringing forth the optimization principle of plasma source design in very low magnetic fields. © *2004 American Institute of Physics*. [DOI: 10.1063/1.1815071]

The helicon-wave discharge has been extensively investigated because a high electron density (10^{12}–10^{13} cm^{-3}) is obtained with comparative ease under a low gas pressure of a few hundreds mPa,[1,2] being used as a plasma source for applications to material processings,[3,4] such as etching, plasma chemical vapor deposition, etc. Conventional helicon-wave discharges need strong magnetic fields ($B_0 \gg 10$ mT) generated by electromagnets with a measurable amount of power, which is inconvenient from the commercial point of view in operating plasma sources with the lower running cost. For the purpose of expanding application fields of the helicon-wave source, it is significant to exploit an operation region where an efficient plasma production is performed in a very low magnetic field. In several previous works concerning the mechanism of the plasma production with anomalously high density,[5–7] on the other hand, a density increment likely attributed to the helicon-wave behavior has been observed under a weak magnetic-field strength much smaller than the magnetic-field strength where the mode transition from an inductively coupled discharge to the helicon-wave discharge appears. However, the reason why the helicon waves can be excited within narrow limits of the low magnetic field has not been exhibited at all. Chen[8] recently suggested using a numerical code that the density peak observed in the low magnetic field is caused by an increase in the plasma loading, which is due to the reflection of a wave at the endplate near the antenna. But, this effect is noticeable only in the case of loop antenna with the azimuthal mode number $m=0$, while the density peak was also observed in other experiments using the $|m|=1$ antennas. Therefore, it is urgently required to systematically investigate the density peak phenomenon, which leads to the clarification of its mechanism and the finding of an available method for efficient plasma production in the region of low magnetic fields.

In this letter, we claim the availability of the helicon-wave discharge even in low magnetic fields below 10 mT by using three types of $|m|=1$ helicon-wave antennas, a phased multiple helical antenna (PMH), a half-wavelength helical antenna (HH),[9] and a double half-turn antenna (DHT).[5] Since PMH is possible to excite spatiotemporally rotating electromagnetic fields with fixed wave numbers parallel and perpendicular to the magnetic-field lines in a plasma, the helicon-wave behavior can be clarified even in the magnetic field lower than the threshold field, above which the conventional helicon wave is excited. A special emphasis is placed on the experimental relationship between the density peak and the antenna configuration in comparison with the the helicon-wave dispersion relation.

The experiment is performed in a pyrex discharge tube with the inner diameter of 9.3 cm and the length of 40 cm, which is connected to a stainless-steel vacuum chamber with the inner diameter of 26.3 cm and the length of 89 cm, as shown in Fig. 1(a). An endplate is set at $z=59$ cm, and the argon gas is fed from a tube end at the gas pressure of $P_{\mathrm{Ar}}=5\times10^{-2}$ Pa. A uniform magnetic field B_0 below 11 mT is applied along the z axis by solenoidal coils. The negative sign of B_0 denotes that the direction of the magnetic-field lines corresponds with $-z$ direction. The helicon-wave antenna with $|m|=1$ is set on the outer surface of the tube. PMH consists of four elements, each of which is one-turn helical conductor wound in the left-hand direction along the $+z$ axis with the length $\ell_z=20$ cm. Figure 1(b) shows the diagram of a radio-frequency (rf) power supply system. rf signals phased temporally through a phase shifter are supplied to two pairs of the antenna elements, each of which is divided into two branches and transmitted to the opposite terminals of the two elements spaced azimuthally 180°. When the phase difference of the rf signals is set 90°, the spatiotemporally rotating rf fields with the azimuthal mode number $|m|=1$ are generated by PMH. The temporal rotation is fixed in the right-hand direction with respect to the $+z$ direction, and the change from $m=+1$ to $m=-1$ is attained by reversing the magnetic-field direction from $B_0>0$ to $B_0<0$. In addition to PMH, HH ($\ell_z=20$ cm), and DHT are also used as the conventional helicon-wave antennas with $|m|=1$, each of which is supplied with the rf power using only one transmission line. The rf frequency is $\omega/2\pi=13.56$ MHz and the rf power is $P_{\mathrm{rf}}\leqslant2000$ W. Plasma parameters and magnetic fluctuations are measured by an axially movable (z axis) Langmuir probe and a magnetic probe, respectively.

Figures 2(a)–2(c) give the electron densities depending on the magnetic field for several rf powers in the cases of using PMH, HH, and DHT, respectively. In the case of PMH, the electron density increases with increasing in B_0 for

[a]Electronic mail: genta@ecei.tohoku.ac.jp

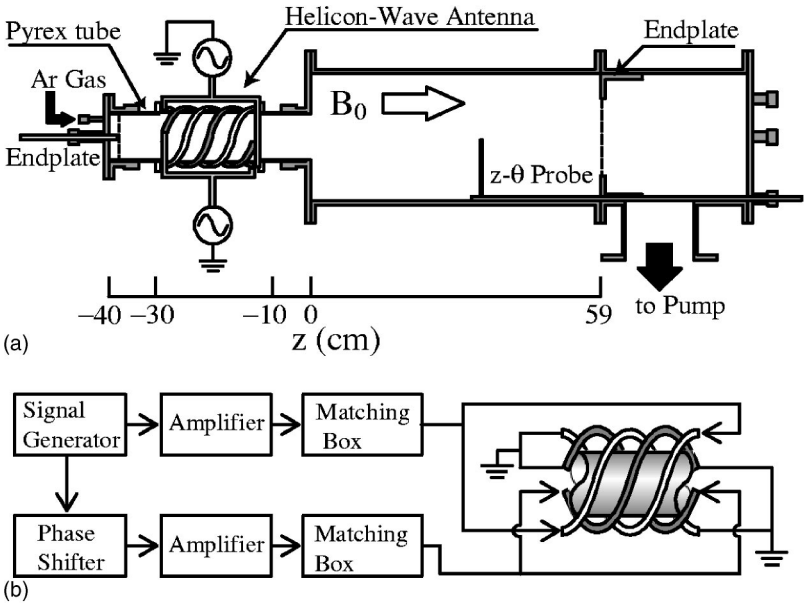

FIG. 1. Schematic diagrams of (a) experimental setup and (b) rf power supply system for PMH.

$m=+1$, and the density has a peak at $B_0 \sim +5$ mT for 2000 W, where the density attains up to one order of magnitude larger than that at $B_0=0$ mT, i.e., inductively coupled plasma mode. The peak density becomes higher with increasing in P_{rf}, and B_0 yielding the density peak is different between each rf power. On the other hand, the density scarcely increases for $m=-1$, and the peak density is almost one-fifth of the magnitude of that for $m=+1$. The density difference between $m=+1$ and $m=-1$ becomes small in the case of HH [Fig. 2(b)] and, furthermore, is not observed in the case of DHT as shown in Fig. 2(c). The reason for the density increment for $B_0<0$ is that DHT concurrently excites $m=\pm 1$ fields, and $m=+1$ field excited regardless of magnetic-field direction gives rise to the density peak. Since HH includes double half-turn parts at the both ends and excites $m=\pm 1$ fields, the density increment is caused for $B_0<0$ [Fig. 2(b)], which is far larger than that in the case of PMH.

When the z component of the magnetic fluctuation, B_z, is measured in the region of $z>0$ cm, waves with a large amplitude are observed to propagate toward the downstream.

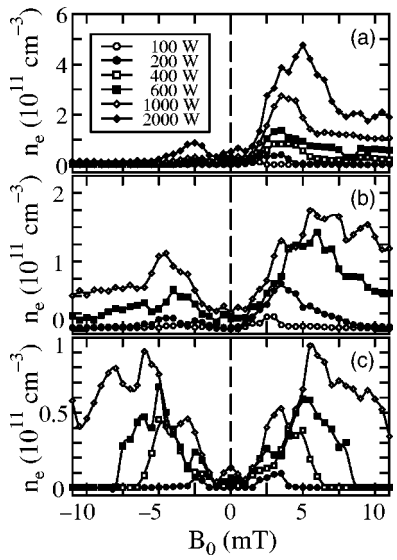

FIG. 2. Electron density depending on magnetic field for various rf powers P_{rf} with (a) PMH, (b) HH, and (c) DHT.

The theoretical dispersion relation of waves has been expressed for a cold uniform plasma:

$$Pn_z^4 + (n_\perp^2(S+P) - 2PS)n_z^2 + (Sn_\perp^2 - RL)(n_\perp^2 - P) = 0, \tag{1}$$

where P, S, R, and L are followed by Stix notation.[10] n_z and $n_\perp$ are the refraction indexes parallel and perpendicular to B_0, respectively. The radial profile of B_z obtained experimentally is almost fitted to the first Bessel function J_1 for the $m=1$ mode, and consequently the perpendicular wave number $k_\perp$ is calculated to be 58 m^{-1} using the relation of $k_\perp = J_1/r$ under the assumption of $B_z=0$ at the plasma edge ($r=6.5$ cm). Figure 3 shows the dispersion relations of the helicon wave (k_z versus ω_{ce}/ω, $\omega_{ce}/2\pi$: Electron cyclotron frequency), which are measured (closed circles) and calculated (solid line) with n_e depending on B_0 for PMH at $P_{\mathrm{rf}}=1000$ W [Fig. 2(a)]. The measured dispersion relation is consistent with the theoretical curve of the helicon wave in the range of $\omega_{ce}/\omega>4$ ($B_0>2$ mT), while that differs in the range of $\omega_{ce}/\omega<4$. Open circles indicate the maximum amplitude of B_z depending on B_0, which is extremely small for $\omega_{ce}/\omega<4$. Hence, the discrepancy of the dispersion relation for $\omega_{ce}/\omega<4$ is caused by the influence of antenna near fields rather than the helicon wave which strongly damps.

When the electron density and the magnetic field are given, the wavelength allowed to exist in the plasma can be calculated by using the dispersion relation. Thus, the rela-

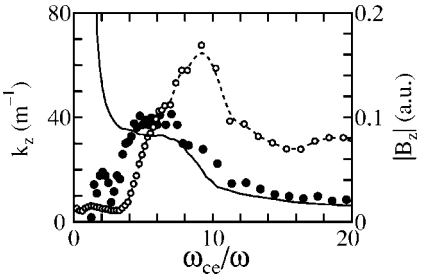

FIG. 3. Dispersion relations of helicon wave measured (●) with PMH at $P_{\mathrm{rf}}=1000$ W and calculated (solid line). The maximal amplitude of axial magnetic fluctuation (○) has a peak around $\omega_{ce}/\omega \sim 10$.

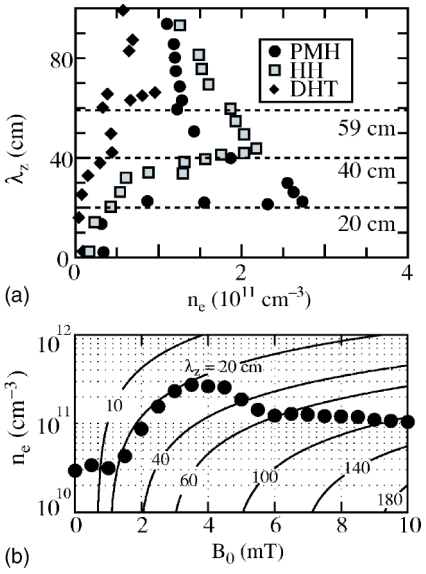

FIG. 4. (a) Relationships between electron density and wavelength at $P_{rf}=1000$ W for PMH, HH, and DHT. (b) Contours of constant wavelength in magnetic field–density plane. Closed circles indicate the density depending on magnetic field with PMH at $P_{rf}=1000$ W.

tionships between the electron density n_e and the axial wavelength λ_z for $P_{rf}=1000$ W are presented in Fig. 4(a), where we use Fig. 2 and Eq. (1) with $\lambda_\perp$ fixed by the radial boundary as mentioned above. The electron density is found to become high at a specific wavelength, i.e., $\lambda_z=20$ cm (40 cm) for PMH (HH). Those wavelengths correspond with one axial wavelength of PMH (ℓ_z) and HH ($2\ell_z$), respectively. In a B_0-n_e plane, the constant λ_z can be depicted as lines in Fig. 4(b). Here, closed circles are the same as Fig. 2(a) for $P_{rf}=1000$ W, which change along the line of $\lambda_z=20$ cm with increasing B_0. The density begins to increase around $B_0=1$ mT, where the density achieved without the helicon wave ($\sim 3\times 10^{10}$ cm^{-3}) intersects the line ($\lambda_z=20$ cm) matching the antenna length. Moreover, an excessive increase in B_0 gives rise to the discrepancy between λ_z and ℓ_z because the density is restricted by the quantity of neutrals and the rf power, and resultantly prohibited to increase with increasing B_0 so as to satisfy the dispersion relation. Therefore, it is found that the helicon wave is excited strongly in the plasma as the wavelength λ_z determined by the electron density and the magnetic field becomes comparable to the one wavelength of the antenna. This finding means that mapping the n_e-B_0 contour as a function of ℓ_z yields the optimum B_0 for the effective plasma production in low magnetic fields. As shown in Fig. 4(a), on the other hand, we can recognize no clear-cut relationship between λ_z and n_e for the DHT case, since the fixed wave number with the z component is hardly excited by DHT. Instead, the density is observed to slightly increase around $\lambda_z=59$ cm corresponding with the chamber length, which is considered due to the standing-wave excitation.[11]

In summary, we have clarified a practical aspect of the helicon-wave discharge employing various $|m|=1$ antennas in magnetic fields much lower than the ordinary magnetic field where the density jump occurs. It is found that the effective excitation of the helicon wave and the efficient plasma production causally take place even in the very weak magnetic field when the axial wavelength of the phased helical antenna launching spatiotemporally rotating electromagnetic fields is matched to that of the helicon wave determined by the plasma dispersion relation. Thus, the optimum magnetic-field strength can be estimated in a plasma source design to obtain the highest density in the region of very low magnetic fields.

The authors would like to thank H. Ishida for technical support, and Y. Sakawa, K. P. Shamrai, F. F. Chen, N. Hershkowitz, and R. W. Boswell for valuable suggestions. This work was supported by Tohoku University 21st Century COE (Center Of Excellence) Program.

[1] R. W. Boswell and F. F. Chen, IEEE Trans. Plasma Sci. **25**, 1229 (1997).
[2] F. F. Chen and R. W. Boswell, IEEE Trans. Plasma Sci. **25**, 1245 (1997).
[3] R. W. Boswell and D. Henry, Appl. Phys. Lett. **47**, 1095 (1985).
[4] C. Charles, G. Giroultmatlakowski, R. W. Boswell, A. Goullet, G. Turban, and C. Cardinaud, J. Vac. Sci. Technol. A **11**, 2954 (1993).
[5] A. W. Degeling, C. O. Jung, R. W. Boswell, and A. R. Ellingboe, Phys. Plasmas **3**, 2788 (1996).
[6] T. Lho, N. Hershkowitz, J. Miller, W. Steer, and G. H. Kim, Phys. Plasmas **5**, 3135 (1998).
[7] D. D. Blackwell, T. G. Madziwa, D. Arnush, and F. F. Chen, Phys. Rev. Lett. **88**, 145002 (2002).
[8] F. F. Chen, Phys. Plasmas **10**, 2586 (2003).
[9] T. Shoji, Y. Sakawa, S. Nakazawa, K. Kadota, and T. Sato, Plasma Sources Sci. Technol. **2**, 5 (1993).
[10] T. H. Stix, *Theory of Plasma Waves* (McGraw–Hill, New York, 1962).
[11] J. P. Rayner and A. D. Cheetham, Plasma Sources Sci. Technol. **8**, 91 (1999).